Self-assembly of amphipathic ααβ-tripeptide into cationic spherical particles for intracellular delivery

Raffaella Bucci, [§a] Priyadip Das, [§b,c] Filomena Iannuzzi,[d] Marco Feligioni,[d,e] Raffaella Gandolfi,[a] Maria Luisa Gelmi,[a] Meital Reches*[b] and Sara Pellegrino*[a]

[a] University of Milano, Department of Pharmaceutical Sciences, Milano, Italy
[b] The Hebrew University of Jerusalem, Institute of Chemistry, Jerusalem, Israel
[c] SRM University, SRM Nagar, Department of Chemistry, Potheri, Kattankulathur, Chennai, Tamil Nadu, India.
[d] Laboratory of Neuronal Cell Signaling, EBRI Rita Levi-Montalcini Foundation, Rome, Italy
[e] Department of Neurorehabilitation Sciences, Casa Cura Policlinico, Milan, Italy

Abstract

The development of molecular carriers able to carry molecules directly into the cell is an intense area of research. Cationic nanoparticles are effective delivery systems for several classes of molecules, such as anticancer agents, oligonucleotides and antibodies. Indeed, the cationic charge on the outer surface allows a rapid cellular uptake together with the possibility to carry negative charged molecules. In this work, we studied the self-assembly of an ultra-short ααβ-tripeptide containing the L-Arg-L-Ala sequence and an unnatural fluorine substituted $\beta^{2,3}$-diaryl-amino acid. The presence of the unnatural $\beta^{2,3}$-diaryl-amino allowed to obtain a protease stable sequence. Furthermore, the Arginine guanidinium group triggered the formation of spherical assemblies that are able to load small molecules and enter cells. These spherical architectures thus, represent interesting candidates for the delivery of exogenous entities directly into cells.

Introduction

The search of new approaches to carry exogenous entities (e.g. drugs, proteins, oligonucleotides siRNA) directly into cells is a very active research field. Nanoparticles have been recently considered as a new efficient method to introduce exogenous entities into cells.[1] Lately, also exosomes, biological microvesicle released from cells, are considered potential new carriers.[2] Cationic nanoparticles (NP^+) are positively charged nanoaggregates that are widely employed in biomedicine,[3] pharmaceutical technology[4] and antimicrobial science materials.[5] NP^+ are being used as effective nano-size delivery systems for different molecules such as anticancer agents,[6] oligonucleotides,[7] antibodies,[8] and proteins.[9]

A wide variety of cationic polymers self assembles into $NP^{+,}$ and most of them are characterized by the presence of basic functions on the surface. This includes amines or guanidines.[3,4,10] NP^+ can be also obtained by the functionalization of anionic or neutral polymers with cell penetrating peptides, *i. e.* positively charged oligopeptides composed mainly by Arginine and/or Lysine residues.[11-16] In all cases, the polymer is the molecular tool that direct the process of self-assembly while the cationic charge decorates the NP^+.

The positive charge on the surface of NP^+ gives several advantages over anionic or neutral systems. First, it allows a rapid cellular uptake through the direct translocation across cell membranes.[17] Furthermore, it enables NP^+ to deliver active macromolecules of negative charge such as DNA or proteins.[7-9]Yet, polymeric NP^+ suffer several drawbacks such as aggregation, instability and cytotoxicity, related not only to the positive surface charge but also to the size and geometry of the constructs.[3,18]

In the last decade, natural biopolymers, such as oligosaccharides, oligonucleotides, and proteins have been widely exploited for the development of new smart materials.[19] In this context, a significant attention has been given to peptides due to their modular nature and structural diversity, biocompatibility, relative chemical and physical stability, and synthetic accessibility.[20,21] Furthermore, peptides can hierarchically self-assemble in a reproducible way through free-energy driven processes, e.g Van der Waals, electrostatic, hydrogen bonding, hydrophobic interactions and π-π stacking interactions.[21] The balance of these forces affects their arrangement that depends on molecular composition, assembly and environment (pH, solvent, temperature, and ionic strength). An added value of peptides is the possibility to introduce unnatural amino acids expanding thus the scope of the resulting nano-architectures together with the obtainment of more proteolitically stable materials.[22] In particular, short peptides and peptide mimics are themselves profitable delivery systems as they could bring both features, *i. e.* self-assembly and cell penetration, into a single molecule, and because of their biocompatibility and low toxicity.[23]

In our group, we recently developed proteolitically stable peptide nanotubes **D2**, composed by L-Ala and an unnatural fluorine substituted $\beta^{2,3}$-diaryl-amino acid.[24] This nanotubular architecture is obtained by intermolecular hydrogen bonds, and van der Waals interactions leading mainly to hydrophobic constructs. Here, we explored the possibility of using the above unnatural amino acid for obtaining cationic construct. The balance between hydrophobicity and charge is crucial for both colloidal stability and membrane penetration.[25] We thus envisaged to introduce an L-Arg residue in the hydrophobic L-Ala-$\beta^{2,3}$diaryl **D2** structure. In this way, a polar interaction could drive the self-assembly, while the cationic guanidium group on the side chain of Arg could influence the shape as well as the overall superficial charge of the aggregates. As a result, we report the development of cell penetrating cationic nanoaggregates composed by an ultra-short ααβ-tripeptide **T2R** (Figure 1) that are able to deliver small molecules into the cell.

Figure 1. Chemical formula of compound **T2R**.

Results and Discussion

Compound **T2R** was prepared starting from known dipeptide **D2**[21] (Scheme 1). First, the N-terminus of **D2** was Boc-deprotected with TFA in CH_2Cl_2. The coupling of **N2** with N-Boc-Arg was performed using EDC and Oxyma[26,27] as coupling reagents and DIEA as the base (24h at rt, 85% overall yield).

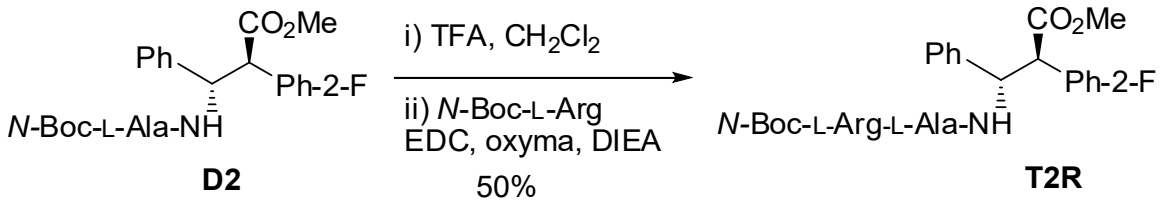

Scheme 1. Synthesis of ααβ-tripeptide **T2R**

Compound **T2R** was characterized by ^{1}H-NMR (17 mM solution, CD_3CN, 293 K, 300 MHz, see Supporting Information). **T2R** was present in solution as a single extended conformer, in which the $\beta^{2,3}$-diaryl-amino acid is characterized by a *trans* configuration according to $^3J_{C\beta H\text{-}C\alpha H}$ values (11.3 Hz). The NOESY experiments (t_{mix} 300 ms) showed a complete set of NH-C_αH (i, i+1) spatial proximities, while no NH-NH (i, i+1) NOE effects were observed. Furthermore, the ^{1}H-NMR experiments at variable temperatures excluded the presence of any intramolecular hydrogen bonds.

The self-assembly tendency of **T2R** was then investigated. According to the protocol already set up for compound **D2**,[24] a stock solution of **T2R** in hexafluoroisopropanol, HFP (100 mg/mL) was diluted with water to a final concentration of 2mg/mL. After an incubation of 24h, the sample was characterized. Dynamic light scattering (DLS) analysis revealed the formation of aggregates with an average diameter of 675 ± 30 nm (see Supporting Information). Scanning electron microscopy (SEM) and Transmission electron microscopy (TEM) showed that **T2R** self-assembled in aqueous

medium into highly ordered spherical particles with nanomeric dimensions. (Figure 2) In particular, high-resolution SEM revealed that **T2R** could form spherical assemblies. Low magnification SEM images demonstrated that these spherical assemblies are abundant. In addition, some of the spheres seemed connected, while others stood as distinct entities.

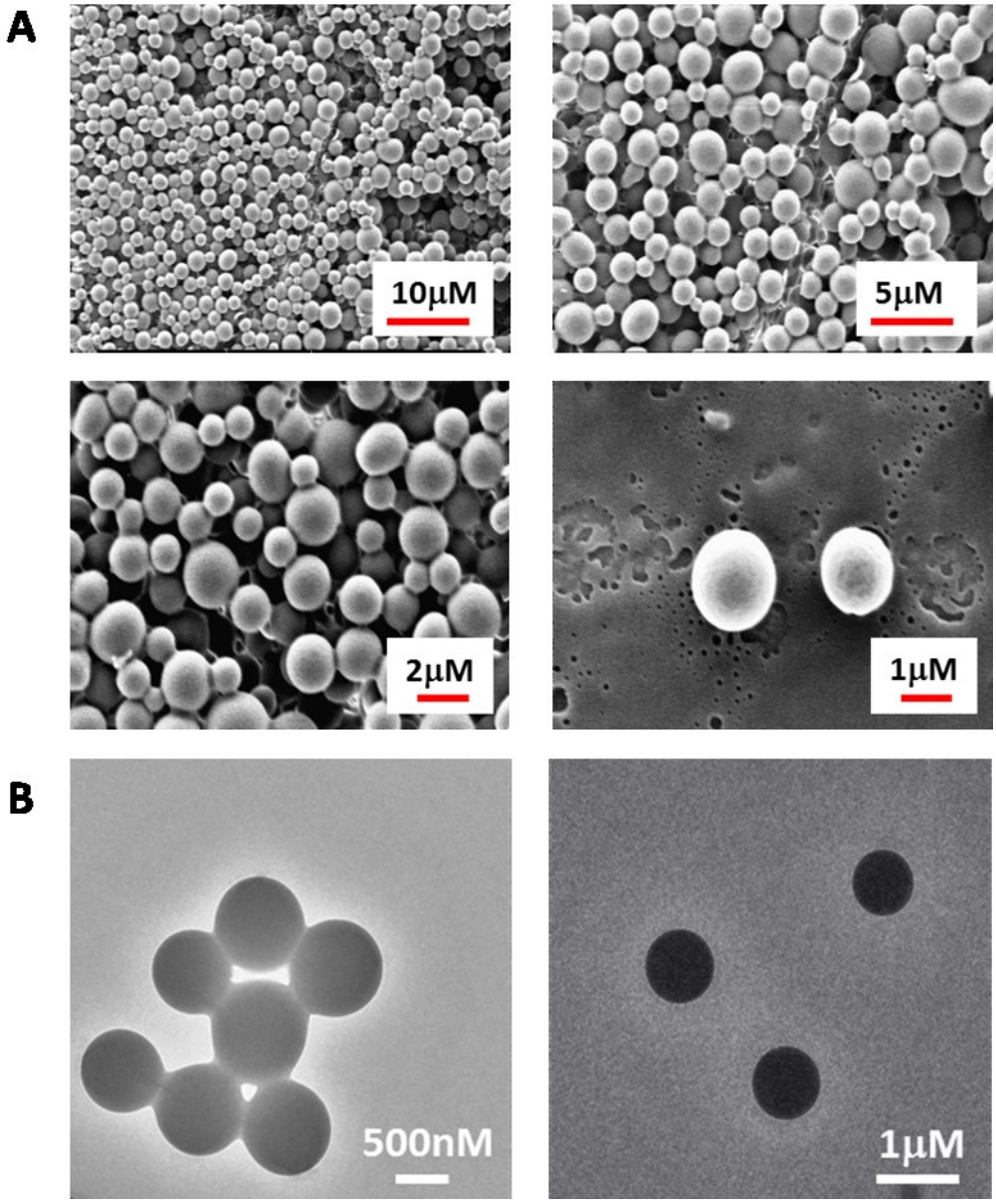

Figure 2. Electron microscopy micrographs of the self-assembled structures formed by **T2R** A) HR-SEM and B) TEM micrographs of**T2R** self-assembled structures**.**

To get an insight into the secondary conformation of the self-assembled spherical structures formed by **T2R** in aqueous medium, we used Fourier transform infrared (FT-IR) analysis and deconvoluted each spectrum. The FT-IR spectra of the spherical structures exhibited major peaks at 1625 cm^{-1}, 1685 cm^{-1} and 1738 cm^{-1}. (Figure 3) The peak at 1738 cm^{-1} corresponds to the ester function. The

appearance of two major peaks in the amide I region at 1625 cm^{-1} and 1685 cm^{-1} may suggest an anti-parallel β-sheet conformation of **T2R** in the aggregates[28].

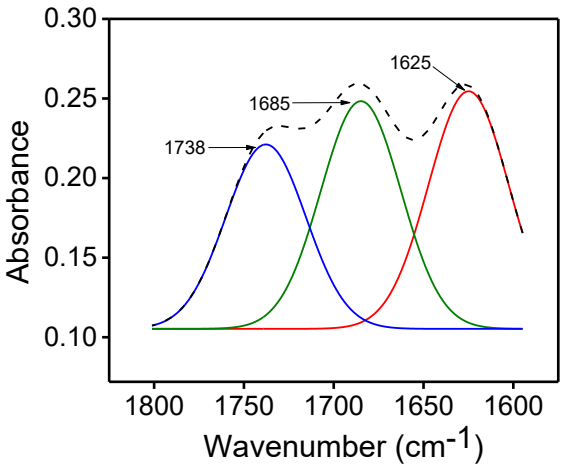

Figure 3. Deconvoluted FT-IR spectra of the self-assembled structures formed by **T2R**. The dashed-line indicates the original FT-IR spectra and the solid line represents the deconvoluted curves with a Gaussian function.

The zeta potential of **T2R** assemblies was +34.7 mV ±0.4 (see Supporting Information) confirming that the protonated guanidinium group is present on the outer sphere surface.

The protease stability of **T2R** was studied using Pronase from *Styreptomyce griseus*, *i. e.* a mixture of endo- and esopeptidase able to hydrolyze standard peptide bonds. In our previous work, we found that Pronase is ineffective in cleaving the amide bond of the unnatural **D2** dipeptide.[24] Solutions of **T2R** (PBS buffer with $CaCl_2$, pH 7) in the presence or absence of Pronase were incubated at 25°C and monitored by RP-HPLC. Different Pronase concentrations were tested (0,5-1-10 mg/ml) maintaining the same **T2R** concentration (5mg/mL). The complete hydrolysis of L-Arg-L-Ala- amide bond was observed only in the presence of high concentration of the enzyme (10 mg/mL) and after 3h (Figure 4). On the contrary, with 1 mg/mL of Pronase, the complete hydrolysis was obtained only after 24 h. Using 0.5 mg/mL of enzyme the total conversion did not occur (Figure 4 and Supporting Information).

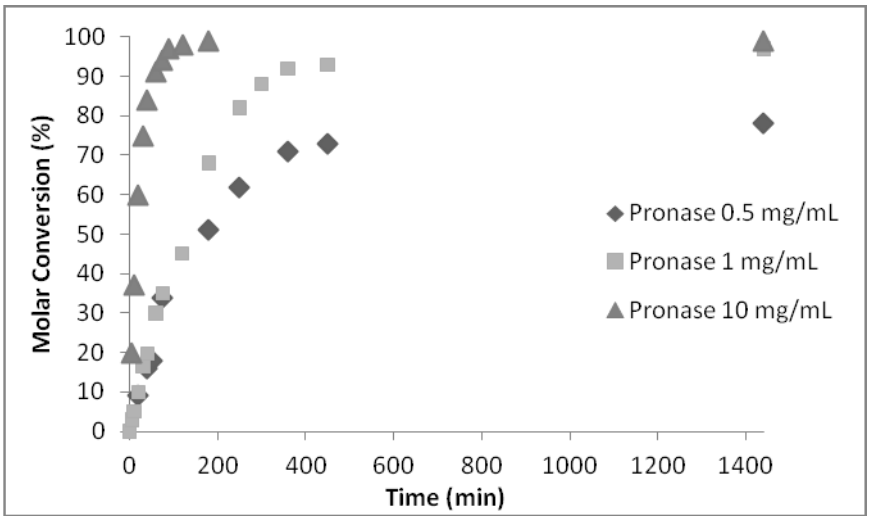

Figure 4. Protease stability analysis of **T2R** (5 mg/mL) using different concentrations of Pronase from *Styreptomyces griseu.*

To evaluate the potential of the spherical assembly formed by **T2R** to serve as a drug-delivery system, we self-assembled **T2R** in the presence of the dye rhodamine B (RhB). The incorporation of RhB was conducted during the **T2R** self-assembly, affording **RhB-T2R** in which the luminescent dye is incorporated within the aggregates. The fluorescence microscopic images of **RhB-T2R** are shown in Figure 5, indicating the loading of the RhB dye onto the spherical structures. **T2R** calculated encapsulation efficiency (EE) was of 56.5%, while loading capacity (LC) was of 13.5% (see Materials and Methods)

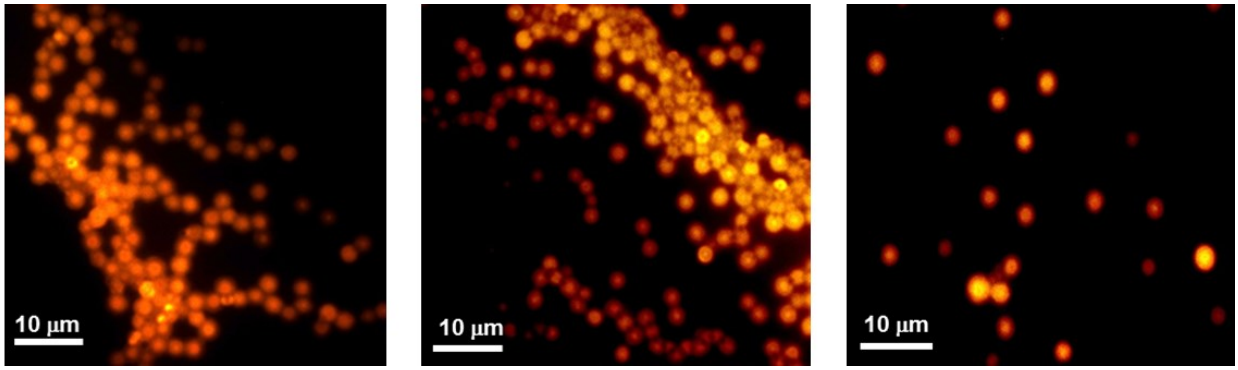

Figure 5. Fluorescence microscopy images of **RhB-T2R**

The release profile of the dye from **T2R** was then assessed using fluorescence measurement analyses. **RhB-T2R** was dispersed in PBS and transferred into a dialysis bag (MWCO 3kDa), immersed in PBS buffer at room temperature. Aliquots were analyzed at different time intervals for 10 days. The fluorescence measurements revealed that there is a steady increase in the emission intensity with increasing time (Figure 6A). Indeed, the concentration of the dye in the buffer (outside the dialysis bag) slowly increased with time. This is due to the release of the dye molecules

from the self-assembled nanostructures. In particular, up to 114 hours (4.75 days), there was a steady/gradual increase in the emission intensity (measurements every hour, then every 4 hours). After, by analyzing the fluorescence with a time intervals of 8 and 12 hours, we did not observe any significant increase in the emission intensity, indicating that the release process was completed and reached equilibrium. To confirm this hypothesis, we followed the dialysis system for a longer time (36 hours) and observed a significant increase in the emission intensity. The emission reached a plateau after 190 hours (7.9 days) (Figure 6B).

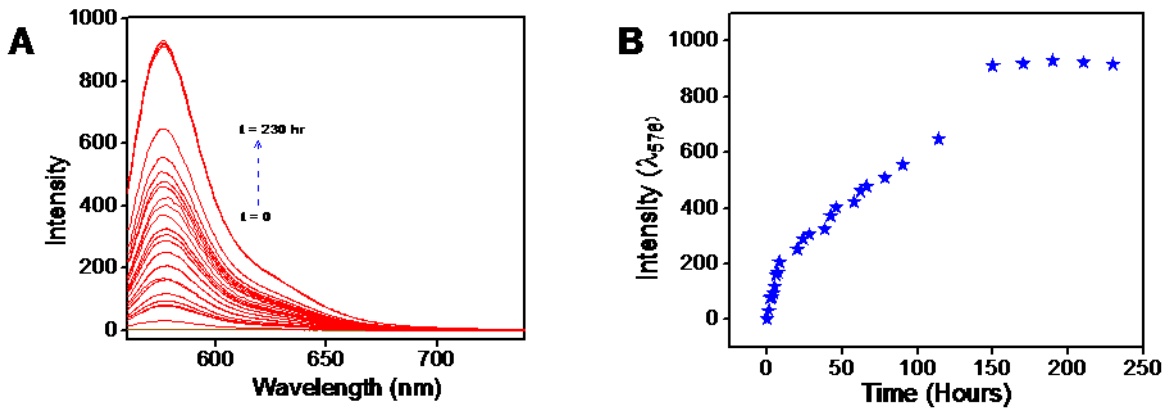

Figure 6: (A) Emission spectra of the PBS buffer solution outside the dialysis bag (contains the RhB-incorporated peptide self-assembled spheres) taken at different time intervals for 10 days. (B) The plot of measured emission intensity of the PBS buffer solution outside the dialysis bag (contain the RhB-incorporated peptide self-assembled spheres) with time; λ_{Mon} = 576 nm, λ_{Ext} = 542 nm.

Finally, the **T2R** aggregates were tested for their cells diffusion capability. HEK-293 cells,[29] a commonly used cell model for the biological research, were treated from 2h up to 16h with 150 μM of **RhB-T2R**. Then, at confocal analyses, the nanoparticles were clearly able to reach the intracellular compartments within the first 2h (Figure 11, Supporting Information) as shown by the bright field image. On the other hand, a very low level of cellular internalization in the florescence channel was observed. Rhodamine fluorescence was instead well visible after 16h, timing that probably allowed a particles enrichment within the cells (Figure 7B). In accordance, the accumulated nanoparticles in the cell after 16h seemed to be in a larger amount (Figure 7E) compared to the detected Rhodamine fluorescence. This difference could be due to the slow dye release property of the self-assembled nanospheres, making this peptide construct particularly interesting as a drug delivery carrier. Moreover, nanoparticles were distributed broadly into intracellular compartments (Figure 7B-C). Interestingly, the nanoparticles could not reach the nucleus as shown by the co-localization between the DAPI and the Rhodamine in which the presence of red dots is not detectable (Figure 7B-C).

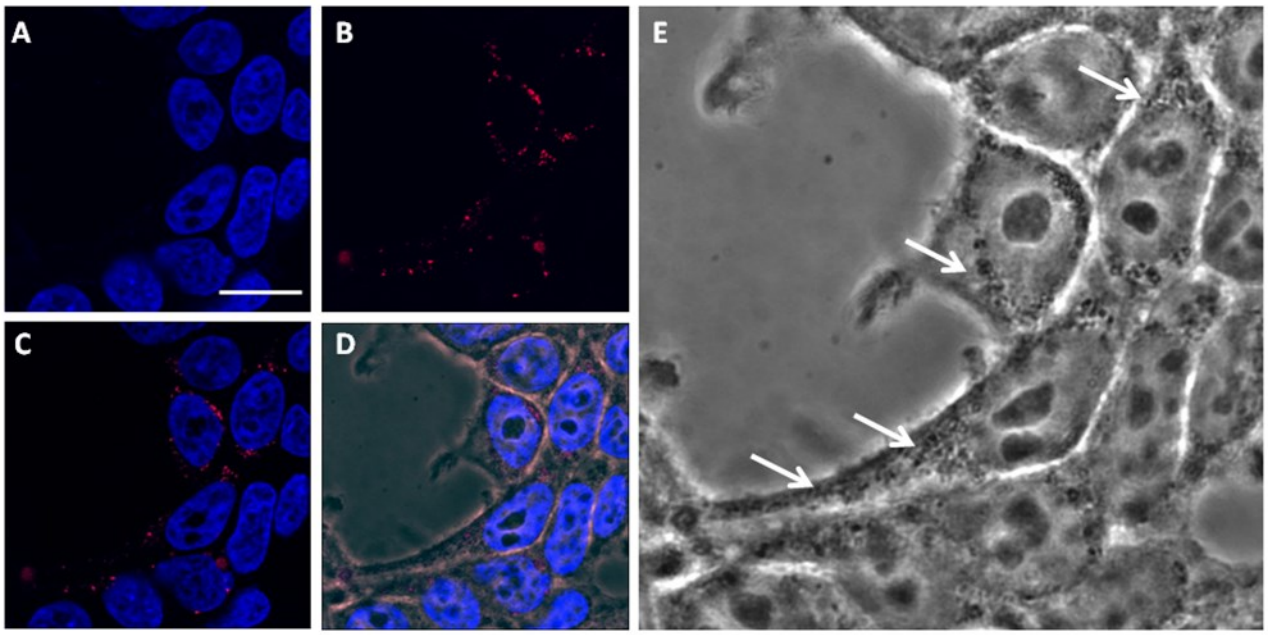

Figure 7. Confocal microscopy images of HEK cells treated for 16 h with **RhB-T2R**culture. A) Representative image of HEK cell culture nuclei stained with DAPI. B) Representative image of **RhB-T2R** in the HEK cells. C) Merged image of DAPI and **RhB-T2R** images. D) Merged image of DAPI, **RhB-T2R** and bright field images. E) Representative bright field image of HEK cells treated with **RhB-T2R**. Particles in the intracellular compartments are indicated by white arrows. Scale bar = 10 µm

Conclusions

In conclusion, the self-assembly of ultra-short ααβ-tripeptide **T2R** that contains L-Arg-L-Ala sequence and an unnatural fluorine substituted $\beta^{2,3}$-diaryl-amino acid have been studied. The presence of Arg guanidinium group on the outer surface triggers the formation of spherical assemblies that are able to load small molecules and enter the cells. Due to the presence of unnatural $\beta^{2,3}$-diaryl-amino, **T2R** positive charged spherical aggregates are proteolitically stable representing thus interesting candidates for the delivery of exogenous entities directly into the cells.

Material and Methods

The reagents and solvents were purchased from Sigma Aldrich and used without additional purification. ^{1}H NMR spectra were recorded at 300 MHz and ^{13}C NMR spectra at 75 MHz using TMS as internal standard. Mass spectra were recorded under electron spray interface (ESI) conditions.

Synthesis of T2R. To a solution of **D2** [24] (100 mg, 0.23 mmol) in CH_2Cl_2 (4 mL) at 0 °C, trifluoroacetic acid (4 mL) was added dropwise. The mixture was stirred for 1 hour at room temperature (TLC, CH_2Cl_2/ MeOH 30:1). The reaction mixture was washed with a saturated solution of $NaHCO_3$ (3 mL) and brine (3 mL). The organic layer was dried on Na_2SO_4 and the

solvent removed. The crude was dissolved in CH_2Cl_2 (1 mL). The solution was cooled to 0 °C. EDC (52 mg, 0.27 mmol), Oxyma[23] (40 mg, 0.27 mmol) were added to a solution of *N*-Boc-L-Arg (82 mg, 0.25 mmol) and the mixture was stirred for 1 h at 0 °C. The mixture of the deprotected dipeptide and DIEA (45 µL, 0.25 mmol) were added. The reaction was stirred overnight at room temperature (TLC, CH_2Cl_2/MeOH 30:1). A saturated solution of NH_4Cl was added. The aqueous layer was separated and organic layer was washed first with a saturated solution of $NaHCO_3$ (4 mL) and then with brine (4 mL) . The organic layer was dried over Na_2SO_4 and the solvent was removed under reduced pressure. The crude mixture was recrystallized from CH_2Cl_2:Et_2O (1:5), affording pure compound **T2R** (127.5 mg, 0.212 mmol, 85% see Supporting Information for complete characterization).

Self-assembly of T2R. A stock solution of **T2R** in HFP (100 mg/mL) was diluted with water to a final concentration of 2 mg/mL. After an incubation of 24 h, the sample was characterized by TEM, and SEM.

***SEM* analysis:** A drop containing 10 µL of the peptides solution was placed on a glass coverslip and allowed to dry at RT. The peptides on the glass were coated with gold.

***TEM* analysis:** A drop containing 10 µL of the self-assembled **T2R** solution, was placed on 200-mesh copper grid, and covered by carbon-stabilized Formvar film (Electron Microscopy Science, PA, USA). After 1.5 min, the fluid in excess was removed from the grid.

Proteolytic stability Enzymatic degradation studies were carried out in PBS buffer (0.01M, pH 7) in the presence of $CaCl_2$ (10 mM). **T2R** (5 mg/mL) was incubated at 25°C under magnetic stirring in absence or in presence of Pronase from *Streptomyces griseus* (0-0.5-1-10 mg/mL). Aliquots (50 µL) of the sample were analyzed at different times from 0 h to 24 h. The reaction was quenched adding 10 µL of acetic acid (25% v/v) and 150 µL of a mixture H_2O:MeCN (60:40). The degradation of **T2R** was monitored by RP-HPLC (Phenomenex LUNA 5µ C18 250 x 4.60 mm) using as eluents 60% water with 0.1% TFA and 40% MeCN (flow rate of 0.8 mL/min). Detection was performed by UV measurement at 220 nm. To evaluate the stability of the enzyme, 1 mg/mL of protease was stirred at 25°C. After 24 h, 5 mg/mL of **T2R** was added and aliquots were analyzed as previously described.

Dye Labeling of T2R Self-assembled Spheres The incorporation of RhB was conducted during the **T2R** self-assembly. RhB at concentration of 10^{-3} mol L^{-1} was added to the **T2R** (dissolved in HFP, initial concentration 100 mg/mL) + TDW H_2O (Final concentration of **T2R** 2 mg/mL). Then the mixture was left for overnight. This mixture leading to the spontaneous accommodation of the dye within the nanospheres (**RhB-T2R**).

Dye Encapsulation Efficiency (EE) and Loading Capacity (LC): RhB-T2R spheres were prepared as reported above, and left to precipitate overnight. The aqueous medium was decanted and the emission intensity at desired wavelength was measured. The dye encapsulation efficiency (EE), which is correlated with the concentration of the dye not incorporated or free unentrapped dye, can be expressed by the equation:[30]

$$EE = \frac{Actual\ concentration\ of\ the\ dye\ incorpoarted\ in\ nanoparticles}{Concentration\ of\ the\ theory\ amount\ of\ dye\ loaded\ in\ nanoparticles} \times 100\%$$

As the concentration of the dye is directly proportional to emission intensity

$$EE = \frac{Emisssion\ intensity\ of\ the\ dye\ incorpoarted\ in\ nanoparticles}{Emission\ intensity\ of\ the\ theory\ amount\ of\ dye\ loaded\ in\ nanoparticles} \times 100\%$$

As the emission of the dye incorporated in nanoparticles is equal to the total emission subctracted the emission intenisity of the not incorporated dye, EE can by calculated by:

$$EE = \frac{Emission\ intensity\ of\ the\ theory\ amount\ of\ dye\ loaded - Emission\ intensity\ of\ the\ dye\ not\ incorpoarted}{Emission\ intensity\ of\ the\ theory\ amount\ of\ dye\ loaded} \times 100\%$$

The loading capacity (w/w %LC) can be calculated by the following expression

$$LC = \frac{Amount\ of\ the\ Entrapped\ drug/dye}{Nanoparticle\ weight} \times 100\%$$

The molecular weight of the RhB =479.02, the total volume of the resultant solution used for the dye incorporation study is 1mL and the Final effective concentration of the T2R is 2 mg/mL. The concentration of RhB actually loaded is of 10^{-3} mol L^{-1}. Then the amount of the dye present in 1 ml is 0.48 mg. The amount of the entrapped dye by the nanoparticles is 0.48 × EE = 0.48 × 56.4% =0.2702 mg.

LC= (0.2702/2) × 100% = 13.5%

Dye release study: RhB-T2R spheres were prepared as reported above, and left to precipitate overnight. The aqueous medium was decanted, and the peptide assemblies were re-dispersed in PBS (10 mM NaCl, pH = 7.4, 150 mM). Then, **RhB-T2R** suspension (2 mL) was transferred into a dialysis bag (MWCO 3kDa), and the bag was immersed in 45 mL of PBS, at room temperature. The buffer outside the dialysis bag (1 mL) was taken at different time intervals for 10 days, for fluorescence measurements. The volume of the solution was kept constant by adding 1 mL of the original PBS solution after each sampling. The fluorescence measurements were performed at room temperature using a fluorescence spectrometer. The emission spectra were collected from 555 nm to

750 nm, with an excitation wavelength of 542 nm. The monitoring wavelength is 576 nm for the emission intensity Vs Time plot.

Dynamic light scattering (DLS) analysis and Zeta potential measurement:A stock solution of **T2R** in HFP (100 mg/mL) was diluted with triple distilled water to a final concentration of 2 mg/mL. After an incubation of 24 h, the aqueous solution having the self-assembled structures of **T2R** use for the Dynamic light scattering (DLS) analysis and Zeta potential measurement. DLS analysis and Zeta potential measurement of the self-assemblies were performed using a Nano-zeta sizer (Malvern instruments), model ZEN3600) and these measurement were performed at room temperature 25°C.

Cells culture HEK cells were seeded on coverslip coated with Poly-L-Lysine (50 μg/mL) placed into 6-well plates. Cells seeding concentration was 4 × 105 the day before treatments and they were maintained in complete medium with the following composition: DMEM (LONZA Group LTD, Switzerland) 4.5 g/L glucose, 10 % fetal bovine serum (LONZA Group LTD, Switzerland), 1 % L-glutamine (Invitrogen - GIBCO) 200 mM, 1 % antibiotics penicillin/streptomycin (Invitrogen - GIBCO). Cells were incubated at 37 °C under 5 % CO2.

Cells culture treatment and Immunostaining HEK cells were treated with **RhB-T2R** at 150 μM. 16h after treatment, the cells have been washed two times with Phosphate buffer (PBS) and, immediately after, they were fixed in 4 % (w/v) freshly prepared paraformaldehyde in PBS for 10 min at room temperature. After four PBS washes, cells were permeabilized with 0.1 % (v/v) Triton X-100/PBS for 5 min, washed again and incubated with DAPI (1.0 μg/mL) for 10 min. After other 3 PBS washes, coverslips were mounted on slides with Hydromount™ mounting gel.

Confocal imaging Slides were examined under a confocal laser scanning microscope (Leica SP5, Leica Microsystems, Wetzlar, Germany) equipped with 4 laser lines and a transmitted light detector for differential interference contrast (DIC; Nomarski) imaging. Confocal acquisition setting was identical between slides. Bright field images were also taken.

Acknowledgements This work has been financially supported by Lundbeck A/S, Casa di Cura del Policlinico di Milano (CCPP), and by University of Milano (Piano di sostegno alla Ricerca 2016-LINEA 2.). P. D. acknowledges the support of the Israel Council for Higher Education.

§ R. B. and P. D. equally contribute to this work

Notes and references

1 A. H. Faraji, P. Wipf *Bioorg Med Chem.* **2009**, 17, 2950-2962.

2 X. C. Jiang, J. Q. Gao *Int J Pharm.* **2017**, *521*, 168-177.

3 E. Bilensoy *Exp. Opin. Drug Del.* **2010**, *7*, 795-809.

4 A. Mokhtarzadeh, A. Alibakhshi, M. Hashemi, M. Hejazi, V. Hosseini, M. de la Guardia, M. Ramezani *J. Contr. Rel.* **2017**, *245*, 245116–245126

5 A. M. Carmona-Ribeiro, L. Dias de Melo Carrasco *Int. J. Mol. Sci.* **2013**, *14*, 9906-9946.

6 X. Jin, P. Zhang, L. Luo, H. Cheng, Y. Li, T. Du, B. Zou, M. Gou *Int J Nanomedicine* **2016**, *11*, 4535–4544.

7 S. Sajeesh, J. Y. Choe, T. Y. Lee, D. Lee *J. Mater. Chem. B* **2015**, *3*, 207-216

8 M. Arruebo, M. Valladares, Á. González-Fernández *J. Nanomaterials* **2009**, doi:10.1155/2009/439389.

9 P. Li, G. Shi, X. Zhang, H. Song, C. Zhang, W. Wang, C. Li, B. Song, C. Wang, D. Kong *J. Mater. Chem. B* **2016**, *4*, 5608-5620.

10 J. Ramos, J. Forcada, R. Hidalgo-Alvarez *Chem. Rev*. **2014**, *114*, 367–428.

11 T. Tashima *Bioorg. Med. Chem. Lett*. **2017**, *27*, 121–130.

12 J. Y. Yoon, K.-J. Yang, S.-N. Park, Do.-K. Kim, J.-D. Kim *Int. J. Nanomedicine* **2016**, 11, 6123-6134.

13 F. Selmin, G. Magri, C.G.M. Gennari, S. Marchianò, N. Ferri, S. Pellegrino *J. Pep. Sci.* **2017**, *23*, 182-188.

14. V. P. Torchilin *Adv Drug Deliv Rev*. **2008**, 60, 548-558.

15 A. El-Sayed, I. A. Khalil, K. Kogure, S. Futaki, H. Harashima *J. Biol. Chem*. **2008**, *283*, 23450-23461.

16 R. M. Sawant , J. P. Hurley , S. Salmaso , A. Kale , E. Tolcheva , T. S. Levchenko , V. P. Torchilin *Bioconjugate Chem.* **2006**, *17*, 943–949

17 J. Lin, A. Alexander-Katz *ACS Nano* **2013**, *7*, 10799–10808.

18 E. Blanco, H. Shen, M. Ferrari *Nat Biotechnol*. **2015**, 33, 941-51.

19 Sa. K. Nitta, K. Numata *Int J Mol Sci*. **2013**, 14, 1629–1654.

20 D. Mandal, A. N. Shirazib, K. Parang *Org. Biomol. Chem*. **2014**, *12*, 3544–3561.

21 S. Eskandaria, T. Guerina, I. Totha, R. J. Stephenson *Adv. Drug Deliv. Rev*. **2017**, *110-111*, 169-187.

22 F. Clerici, E. Erba, M. L. Gelmi, S. Pellegrino *Tetrahedron Lett*. **2016**, *57*, 5540-5550.

23 L. Liu, K. Xu, H. Wang, P. K. J. Tan, W. Fan, S. S. Venkatraman, L. Li, Y.-Y. Yang *Nature Nanotechnology* **2009**, *4*, 457–463.

24 A. Bonetti, S. Pellegrino, P. Das, S. Yuran, R. Bucci, N. Ferri, F. Meneghetti, C. Castellano, M. Reches, M. L. Gelmi *Org. Lett*. **2015**, *17*, 4468–4471.

25 J. J. Panda, A. Varshney, V. S. Chauhan *J. Nanobiotec*. **2013**, *11*, 18.

26 R. Subiròs-Funosas, R. Prohens, R. Barbas, A. El-Faham, F. Albericio *Chem. Eur. J.* **2009**, *15*, 9394 – 9403.

27 A. Caporale, N. Doti, A. Sandomenico, M. Ruvo *J. Pept. Sci*. **2017**, *23*, 272–281.

28. J. Kong, S. YU *Acta Biochim. Biophys. Sin.* **2007**, *39*, 549-559.

29 Y.-C. Lin, M. Boone, L. Meuris, I. Lemmens, N. Van Roy, A. Soete, J. Reumers, M. Moisse, S. Plaisance, R. Drmanac, J. Chen, F. Speleman, D. Lambrechts, Y. Van de Peer, J. Tavernier, N. Callewaert *Nature Comm.* **2014**, *5*, 4767.

30. J. Pan, S.-S. Feng *Biomat.* **2006**, *27*, 4025–4033.

31. B.Y. Chu, L. Zhang, Y. Qu, X.X. Chen, J.R. Peng, Y.X. Huang, Z,Y, Qian *Sci. Rep.* **2016**, *6*, 34069.